

OFFICIAL JOURNAL OF THE BRITISH HOROLOGICAL INSTITUTE

The Horological Journal



APRIL 2024
www.bhi.co.uk



How Many Days in an Egyptian Year?

Evidence from the Antikythera Mechanism

Stuart Malin



R. J. Dickens



(1) Introduction

The Antikythera Mechanism – its discovery, history and interpretation – has been well documented (see, for example, Jones, 2017, Freeth *et al*, 2021, or search ‘Antikythera’ on YouTube¹). Here, we are particularly, but not exclusively, concerned with the claim (Budiselic *et al*, 2021², hereinafter referred to as BTDR) that the front dial of the mechanism, specifically fragment C, contains evidence of an Egyptian lunar year.

Fragment C of the Antikythera Mechanism includes some 80 degrees of two concentric annuli. The outer one is known as the calendar ring because it is inscribed in Greek with the names of three Egyptian months; the inner one is known as the zodiac ring (see ‘Figure 1’ of BTDR). The calendar ring is located in a shallow channel in the front dial plate, in which it was, presumably, free to move except when pinned to one of the holes in the channel.

The long-standing assumption, based largely on the fact that it includes named Egyptian months, is that the outer wheel had 365 equal divisions corresponding to the number of days in the Egyptian civil calendar. This assumption has been challenged by BTDR, based on their measurements of X-ray tomographic images of the holes in the channel below the ring, assumed to correspond to the divisions marked on it.

They conclude, with supporting statistical evidence, that the number of divisions, N , is more likely to be 354, which would be the number of days in a lunar year, i.e. 12 lunar months of 29.5 solar days. The number N is of importance for its implications not only regarding the Antikythera Mechanism, but also for the study of ancient calendars.

As outsiders with no preconceptions, we have presumed to re-examine the evidence for the value of N (365, 354, or neither), basing our study purely on the measured positions of the 81 holes.

(2) Mathematical Interlude

The purpose of this section is partly to introduce the terminology and explain the methods used here, but mainly to spell out the details of how we have applied them. If you are already familiar, or don’t want to get involved with this topic, skip this section. It will still be here if you change your mind!

While it is our purpose to determine the best value of N , it is of at least equal importance to accompany N with a reliable estimate of its uncertainty. We make the usual assumption that the errors are normally distributed and quote them throughout as standard errors.

For M independent estimates of equal weight, the standard error of the mean, SEM, is given by $SEM = [SSR/(M(M-1))]^{1/2}$, where SSR denotes the sum of the squares of the residuals. (The reason for emphasising *independent* with italics will emerge in the next section.)

When U unknowns are to be determined simultaneously from M independent observations, each observation provides an equation of condition in the U unknowns. We solve these by the method of least-squares, which involves the formation and inversion of a normal equation’s matrix.

In this case the standard error of each unknown is given by

$$SE = [SSR \times L / (M - U)]^{1/2} \quad (1)$$

where L denotes the term on the leading diagonal of the inverse normal equation’s matrix corresponding to the relevant unknown; the quantity $(M - U)$ is the number of degrees of freedom. For a simple mean, $U = 1$ and L becomes $1/M$, thus reverting to the SEM formula given above.

The least-squares method is described, together with a FORTRAN program for its implementation, by Malin, Barraclough and Hodder³. It can be directly applied only if the equations to be solved are linear, i.e. of the form $A_1.X_1 + A_2.X_2 + A_3.X_3 + \dots = B$, where A_1, A_2, A_3, \dots , and B are numerical quantities, and $X_1, X_2, X_3 \dots$ are the unknowns to be determined.

For non-linear equations, such as those encountered in the present study, for example the equation of a circle of radius R and centre (X, Y) through (x_m, y_m) , $(x_m - X)^2 + (y_m - Y)^2 = R^2$ (see BTDR, p107), we first need to linearise them before solving for X, Y and R .

To do this we approximate R, X and Y by R_0, X_0 and Y_0 , where $R = R_0 + \delta R, X = X_0 + \delta X$ and $Y = Y_0 + \delta Y$.

On the assumption that the approximation is close to the solution, $\delta R, \delta X$ and δY will be sufficiently small that we may disregard terms involving their squares and higher powers.

Substituting in (1), expanding, rearranging and dropping terms in $\delta R^2, \delta X^2$ and δY^2 , we obtain

$$(X_0 - x_m)\delta X + (Y_0 - y_m)\delta Y - R_0.\delta R = 1/2[R_0^2 - (X_0 - x_m)^2 - (Y_0 - y_m)^2].$$

This is a linear equation of the form $A_1.\delta X + A_2.\delta Y + A_3.\delta R = B$, where $\delta X, \delta Y$ and δR are the unknowns to be determined by minimising the sum of the squares of the residuals. Improved estimates of X, Y and R are given by $X_0 + \delta X, Y_0 + \delta Y$ and $R_0 + \delta R$. If the corrections are large, the process can be repeated with the improved estimates of X, Y and R in place of X_0, Y_0 and R_0 , and so on until convergence is achieved.

If convergence is slow, a successive over-relaxation factor (SOR) may be introduced to speed it up.

In combining errors, we use the usual rules that apply when the error is small compared with the quantity with which it is associated (for the relevant quantities here it is typically c. 1%). In particular, the product of $A \pm a$ and $B \pm b$ is taken to be $AB \pm (A^2b^2 + B^2a^2)^{1/2}$ and the quotient as $A/B \pm (A^2b^2 + B^2a^2)^{1/2} / B^2$.

(3) The BTDR Analysis, With Comments

The data of BTDR are the (x, y) coordinates of the centres of the 81 extant holes, which they have provided in the Harvard Dataverse repository⁴. Each datum is the mean of from three to eight measures, repeated until consistency was achieved.

We do not have the means to measure the positions of the holes for ourselves, but it is clear from their description of the process that BTDR have done a careful and thorough job, and to a higher precision (0.00001 mm) than that to which the maker could have aspired.

The holes are assigned by BTDR to eight sections, denoted S0 to S7, divided by apparent mechanical breaks in the dial plate. We do not dispute their division of the holes into these sections. However, in §5, we examine the possibility that the movement between adjacent sections may in certain cases be negligible.

The points are plotted to the nearest 0.1 mm (limited by pixel-size) in **Figure 1** (c.f. BTDR (Figure 2), reproduced below on p145), together with a red circle to illustrate the closeness of fit of all the points to a circle, even without taking account of possible discontinuities between sections.

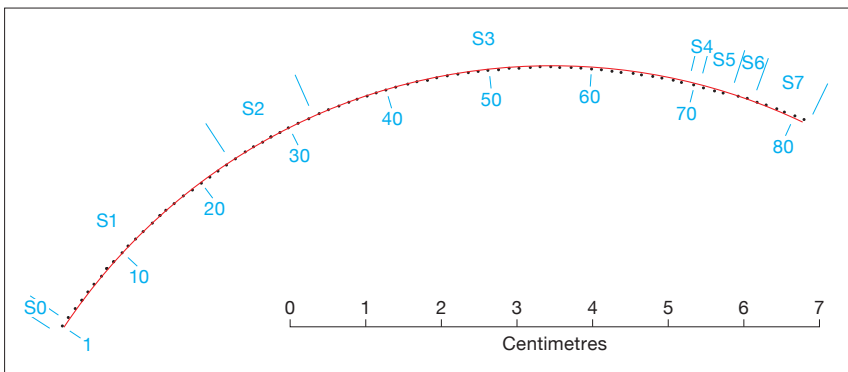


Figure 1. Plot of the (x, y) data of BTDR, pixel-limited here to the nearest tenth of a millimetre. Their hole numbers, 1 to 81, are indicated below the curve and their section-numbers, S0 to S7, above the curve. The red curve is part of a circle of radius 77.5 mm eye-fitted to the curve.

The objective of BTDR was to determine D , the mean distance between adjacent holes, and R , the radius of the circle on which the holes were made. The number of holes, N , in the original circle can then be deduced from the relation

$$N = \pi / \arcsin(D/2R) \quad (2)$$

Values of D have been calculated by BTDR for pairs of holes within sections S1, S2, S3, S5 and within the combined sections S6/S7 (these 74 estimates of D are included in the file with the (x, y) data).

Having re-calculated from scratch, we concur that their mean and standard error of the mean (SEM), as derived by their arithmetical method, is 1.365 ± 0.015 mm. However, we have reservations about their method. The first is that equation (2) is strictly valid only if both holes defining an estimate of D are equidistant from the centre of the circle. If one hole is distant R from the centre and the other at a different distance, whether greater or less than R , D will be overestimated. This small, but systematic effect will inevitably lead to an overestimate of the mean value of D and hence an underestimate of N . This issue is addressed in §5.

The second reservation is that the 74 estimates are not independent (see previous section), since each hole in a section,

other than the two terminal holes, contributes to two estimates. This effect significantly reduces the number of independent estimates, so their SE is underestimated. This effect is quantified in §4.

For their determination of R , BTDR restrict their study to the 37 holes of the largest unbroken section, S3, from which they select triplets of holes whose hole-numbers we denote (a, b, c) where $32 < a < b < c < 70$. They omit those triplets where the chord-length is less than ‘half the width of the arc’, which requires that every triplet should span at least 19 holes.

So:

a can take any value from 33 to 51;

b can take any value from $(a + 1)$ to $(c - 1)$;

and c can take any value from $(a + 18)$ to 69 (inclusive in all cases).

Thus, the total possible number of distinct triplets is 4370, whereas BTDR quote the number of such triplets as being 26,220, which is six times too large. It would appear that they have considered (a, b, c) , (a, c, b) , (b, a, c) , (b, c, a) , (c, a, b) and (c, b, a) as separate triplets.

Their description of their analysis of each triplet is somewhat confusing. We understand the gist of it to be that each triplet provides three equations of the form $R^2 = (X - x_n)^2 + (Y - y_n)^2$, where n takes the values a, b and c . The three equations are solved exactly for the three variables R, X and Y . It is from these values of R, X and Y that they have derived the means and standard errors of these quantities.

From the data given in their ‘Table 1’ and the associated statistics it appears that BTDR have assumed that there are 26,220 independent values, whereas, since the data

for S3 comprise only 37 values each of x and of y , the total number of independent data is 74.

Each equation requires both x and y for hole n so the maximum number of independent equations is $M = 37$.

In determining the three unknowns R, X and Y , a further three degrees of freedom are used reducing the number to $M - 3 = 34$. Thus, it would appear that they have underestimated the SE of their R value by a factor of $(26220/34)^{1/2} \approx 28$.

This would appear to be the basis of their remark (p107, col. 1) that ‘...the extant arc is sufficiently accurate to determine the radius of the original circle’ [and hence its circumference] ‘within a very close approximation’. The importance of this is that the validity of their TOST test is dependent on just such a close approximation.

The effect of the triplet method on the mean value of R is less dramatic, but still worthy of comment. The number of triplets to which a hole contributes varies with hole number. The outermost holes, Nos. 33 and 69, each occur in 494 triplets. Nos. 34 and 68 in 478 triplets, and so on decreasing by 16 with each step towards the central three holes, Nos. 50, 51 and 52, each of which occurs in 222 triplets. This leads to a weighting that changes linearly between the outermost holes and the central one by a factor > 2.2 . Therefore, it is not appropriate to give equal weight to each triplet, as BTDR appear to have done.

For the above reasons, we considered it desirable to do an independent analysis of the data.

(4) Our Analysis

Recognising that the BTDR data are unlikely to be superseded in the foreseeable future, we consider it to be important to extract as much information as possible by using all the data, rather than just S3 and, so far as is possible, to give equal weight to the x and y values for every hole.

Our re-analysis of D is closely similar to that of BTDR, being based on the same set of 74 estimates. The differences are that we equalised the contribution from each hole by giving all the D estimates a weight of 0.5, except the ten that involved the first and last holes in a section, which were given weight 0.75.

The number of independent holes is estimated as follows. By pairing the 1st and 2nd, 3rd and 4th, 5th and 6th, etc holes of a section with an even number of holes, h , it is clear that there are $h/2$ pairs of adjacent holes to which each hole contributes once and only once. When h is odd the number is $(h-1)/2$, with one hole un-paired.

To compensate for this, we allow these odd-holed sections an extra 0.5, thus assigning $h/2$ independent estimates to every section, even or odd, resulting in a total of $M=40$ independent estimates. The weighting also sums to 40 and for similar reasons, but it must be emphasised that the weighting is to adjust the relative rather than the absolute contribution of each estimate; i.e., all the weights could be multiplied by any arbitrary constant without affecting either the mean or the SE. Our revised analysis gives $D = 1.363 \pm 0.021$ mm.

This is only marginally different from BTDR, but with the differences of both mean and SE in the expected directions.

For R , our initial approach is to fit the best circle through the holes of each segment separately. The method is detailed in §2. The method could not be applied to sections with fewer than three holes, and the 3-hole section S5 gave an exact solution, rendering it useless for statistical purposes since it had no error estimates. **Table 1** gives the results for the remaining sections S1, S2, S3 and S7. The final entry is the mean of these four sections, weighted inversely as the square of their SEs.

| | Hole Nos. | R | X_0 | Y_0 |
|-------------|-----------|-------------------|------------------|--------------------|
| S1 | 2–23 | 77.42 ± 0.93 | 79.75 ± 0.65 | 136.09 ± 0.68 |
| S2 | 24–32 | 52.48 ± 2.79 | 68.11 ± 1.33 | 113.79 ± 2.46 |
| S3 | 33–69 | 77.31 ± 0.29 | 79.86 ± 0.04 | 135.67 ± 0.30 |
| S7 | 76–81 | 75.97 ± 20.74 | 83.59 ± 7.23 | 135.09 ± 19.45 |
| S1, 2, 3, 7 | | 77.09 ± 0.28 | | |

Table 1. Means and SEs of R , X_0 and Y_0 (in mm) for sections and for all-values. Hole numbers are inclusive.

By substituting the above values of D and R into equation (2) we obtain $N = 354.8 \pm 5.6$. On the assumption that the holes beneath the calendar ring are a representative sample of those round a uniformly divided circle, and that the holes match the divisions on the calendar ring, the hypothesis that there were 365 of them becomes very unlikely.

The probability that N is 1.8 standard errors greater than 354.8 is only 1 in 28.⁶ The 354-division hypothesis of BTDR, on the other hand, is well within one standard error. If this were a two-horse race, 354 would be the hot favourite and 365 the 28-to-1 outsider.

While this result is persuasive, it is tempting to attempt to extract a little more information from the data.

(5) Further Analysis

From simple geometrical considerations, the calendar ring could have slid in its channel only if both ring and channel were circular (or linear, which is clearly not the case), so R must be the same for each sector.

This important constraint has not been imposed in the foregoing analysis. Neither has the hypothesised constraint that the holes were, as nearly as the maker was able, uniformly spaced around their circle, though that was implicit in the derivation of D . Not all the holes were used (74 of 81) and, because the mean was weighted according to the variance, each hole was not given equal weight.

In an attempt to rectify these deficiencies as far as possible (at this stage, there is no obvious way of incorporating the single-hole sections other than by arbitrarily tagging them onto an adjacent section), we re-state the equations for x_m and y_m in terms of all the unknowns, and solve for them all simultaneously.

We specify the separation between adjacent holes by the angle θ , (see **Figure 2**), rather than D for two reasons:

1. θ is not affected by the tendency to overestimation that affects D (see §3).
2. θ is directly related to N by $N = \pi/\theta$ without needing knowledge of either R or D .

The purpose of the analysis is to determine from the data the best least-squares values of R , θ , α , X_s and Y_s (see **Figure 2**), where s takes the values 1, 2, 3, 5, 6 and 7, corresponding to section numbers.

The data comprise (x, y) values for each hole measured from an arbitrary origin and with arbitrary orientation of the axes. Sections S0 and S4 are omitted because each consists of a single hole. Each x and y contributes an equation of condition, so we have 158 equations to solve for 20 unknowns.

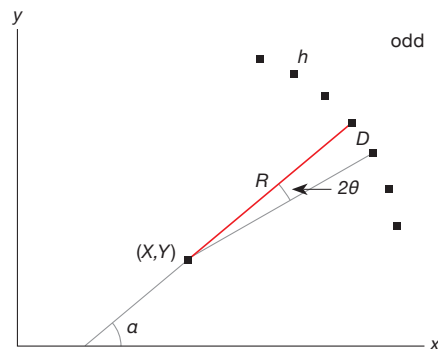


Figure 2A. Sector with an odd number of holes.

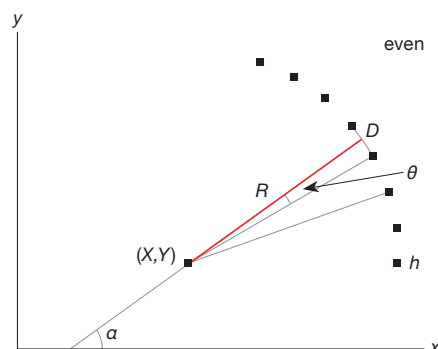


Figure 2B. Sector with an even number of holes.

The geometry of two sections, one with an odd number of holes and one with an even number, is illustrated in **Figure 2**. The bold line is that joining the centroid of the points, (\bar{x}, \bar{y}) , to (X, Y) , where \bar{x} , denotes the mean of all the x 's in the section and \bar{y} the mean of the all the y 's.

The direction of the line is from (X, Y) towards (\bar{x}, \bar{y}) ; it makes an angle α with the x -axis, as shown in **Figure 2**. The angle 2θ subtended at (X, Y) by D is the same for all pairs of adjacent holes in all segments; to a close approximation its value in radians is D/R . (The exact relation is $\theta = \arcsin D/2R$, but, since $\theta \approx 0.5^\circ$, the approximation is in error by less than 13 parts in a million.)

From **Figure 2A** it may be seen that, for hole h , $x = X + R \cos(\alpha + 4\theta)$ and $y = Y + R \sin(\alpha + 4\theta)$, and from **Figure 2B** that $x = X + R \cos(\alpha - 3\theta)$ and $y = Y + R \sin(\alpha - 3\theta)$.

Similar equations may be obtained for all of the holes. In general, for hole h in a section that goes from holes a to b , inclusive, the line joining hole h to (X, Y) is of length R and is at an angle to the x -axis of $\gamma = \alpha + m\theta$, where $m = (2h - a - b)$.

The equations are $x = X + R \cos \gamma$ and $y = Y + R \sin \gamma$.

Linearising these equations by the same process described in §2, we obtain:

$$\cos \gamma \delta R - \sin \gamma R_0 m \delta \theta - \sin \gamma R_0 \delta \alpha + \delta X = x - (X_0 + R_0 \cos \gamma)$$

and

$$\sin \gamma \delta R + \cos \gamma R_0 m \delta \theta + \cos \gamma R_0 \delta \alpha + \delta Y = y - (Y_0 + R_0 \sin \gamma).$$

The importance of choosing realistic initial values, those with subscript $_0$, has already been mentioned. From §4 we know that $D = 1.363 \pm 0.021$ and that N is likely to be either 365 or 354. To avoid favouring either of these options, we select their mean: $N = 359.5$. Since $D/2R = \theta = \pi/N$, this leads to our choice of $\theta_0 = 0.008739$ radians and $R_0 = 78.1$ mm.

For initial values of α , X and Y for the sections, we return to **Figure 2**. We choose α_0 such that $\tan \alpha_0 = -(x_a - x_b)/(y_a - y_b)$, the gradient of the perpendicular bisector of the line joining the first and last points of the sector.

For an odd numbered section, (X, Y) is the point on a line of slope $\tan \alpha_0$ that passes through the middle hole, (x_h, y_h) , where $h = (a + b)/2$, and is distant R_0 from that hole.

The ambiguity in direction is resolved by inspection. For an even numbered section, (x_h, y_h) is replaced with the mean position of the two points closest to the centre of the section. Thus $X_0 = x_h + R \cos \alpha_0$ and $Y_0 = y_h + R \sin \alpha_0$.

The resulting values of α_0, X_0 and Y_0 for each sector are given in **Table 2**, together with the values of α, X and Y obtained from an iterative least-squares solution of the equations of condition. The resulting centres, (X, Y) , are plotted in red on **Figure 3**.

| | Initial estimates | | | After iteration | | |
|---------|-------------------|---------------------|---------|------------------------|-------------------------------------|---------------------------|
| Section | α_0 | X_0 | Y_0 | α | X | Y |
| S1 | 3.94315 | 80.144 | 136.670 | 3.94359 ± 0.00274 | 79.685 ± 0.779 | 136.062 ± 1.492 |
| S2 | 4.21835 | 80.193 | 136.399 | 4.21834 ± 0.01046 | 79.905 ± 0.882 | 135.721 ± 1.238 |
| S3 | 4.62606 | 80.081 | 136.474 | 4.62731 ± 0.00125 | 79.868 ± 0.135 | 135.704 ± 1.115 |
| S5 | 4.97718 | 81.444 | 136.908 | 4.97756 ± 0.05735 | 81.505 ± 4.290 | 136.126 ± 1.007 |
| S6 | 5.02941 | 81.273 | 136.568 | 5.02942 ± 0.11470 | 81.510 ± 8.436 | $135.845 \pm \text{----}$ |
| S7 | 5.07640 | 82.775 | 137.076 | 5.07439 ± 0.01940 | 83.168 ± 1.904 | 136.419 ± 0.395 |
| | R_0 78.1 | θ_0 0.008739 | | R 77.342 ± 1.092 | θ 0.0084335 ± 0.00026544 | |

Table 2. Initial estimates and final values of the all-in-one analysis.

The sum of the squares of the residuals, 1.699 mm^2 , indicates that this 20-variable model provides an excellent fit to the data, with the RMS difference between the model and the individual x and y observations being a mere 0.1mm. However, with so many variables, some of them determined from very few data (for example, for S6, just four equations contribute to the determination of α, X and Y ; S5 is not much better) the conditioning is poor, so it is unsurprising that the standard errors are relatively large. Nevertheless, the solution converges rapidly and stably to the values given in **Table 2**.

These results enable us to examine the relative movements of the different sections. Differences in (X, Y) between sections will indicate a part of such movement, but any rotation of a section about its centre, (X, Y) , will not affect the position of that centre. However, such rotation would be revealed by the values of α .

To illustrate, consider two sections A and B , with mean hole-numbers m_A and m_B and the same centre (X, Y) . If there were no rotation of A relative to B , then the difference $\alpha_A - \alpha_B$ should be insignificantly different from $\Delta = 2\theta(m_A - m_B)$.

In the case of S2 and S3, $(\alpha_A - \alpha_B) - \Delta = -0.021 \pm 0.035$, indicating negligible rotation. The difference between the centres is 0.04mm; again negligible. Thus, we deduce that there has been no significant movement between S2 and S3. This is our justification for combining S2 and S3 into a single set, denoted S23. The corresponding figures for S5 and S6 are also negligible in comparison with their SEs, so we combine them to form S56.

Hole 1 (S0) has no (X, Y) associated with it, but its distance ($D = 1.382$) from hole 2 is well within the range of the 74 other D values, and its distance from the centre of S1 (76.609) is within one SE of R . For this reason, we combine S0 and S1 to form the set S01. Similar evidence from hole 70 is our justification for uniting S4 and S56 to form S456.

We now have reduced the number of sets from 6 to 4: holes 1–23 for S01, 24–69 for S23, 70–75 for S456; and 76–81 for S7. These include all the data and reduce the number of unknowns from 20 to 14, thus improving the conditioning.

The results of analysis, again with the same initial estimates of D and θ that favour neither $N = 354$ nor 365, confirm this by yielding appreciably smaller SEs ($R = 77.057 \pm 0.0796$; $\theta = 0.008896 \pm 0.000093$) with only a marginal increase of root mean square from 0.10 to 0.13mm. The (X, Y) positions are marked in blue on **Figure 3**.

Can we take this process further? The grouping of blue points in **Figure 3** suggest and the numerical data confirm that we may yet further reduce the number of variables from 14 to 8 by combining S01 and S23 into S0-3, and S456 and S7 into S4-7.

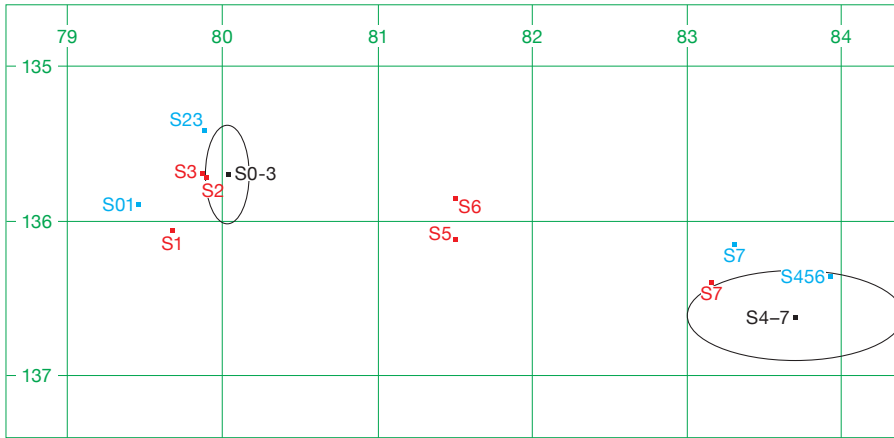


Figure 3. Plots of (X, Y) for each of the sections. Those in red are for the six-section analysis, in blue for the four-section analysis, and black for the (final) two-sectional analysis. The ellipses enclose all points within one standard error of the two-section values.

As before, R and the inter-sector D values are comfortably in range, so there is no evidence of rotation or translation between the segments to be combined. The results are given in **Table 3** and are plotted in black on **Figure 3**, together with ellipses with semidiameters of 1 SE.

This is our final analysis, since there is a significant shift between the two sets, precluding further merging. It is also the model that puts the tightest constraints on θ and hence on \mathcal{N} .

| | Initial values | | | After iteration | | |
|---------|----------------|---------------------|---------|------------------------|-------------------------------------|---------------------|
| Section | α_0 | X_0 | Y_0 | α | X | Y |
| S0-3 | 4.33757 | 80.779 | 136.177 | 4.33949 ± 0.00071 | 80.041 ± 0.136 | 135.698 ± 0.322 |
| S4-7 | 5.01920 | 83.267 | 137.218 | 5.01339 ± 0.00958 | 83.709 ± 0.712 | 136.622 ± 0.294 |
| | R_0 78.1 | θ_0 0.008739 | | R 77.352 ± 0.324 | θ 0.0089163 ± 0.00003875 | |

Table 3. Initial estimates and final results from a two-section analysis.

(6) Summary and Conclusions

From a study of the holes in the faceplate below the calendar wheel of fragment C of the Antikythera Mechanism, BTDR have deduced that there were originally 354 of them. They take this to be the number of days in the calendar used in the Mechanism, as opposed to the traditional belief that it was 365. Despite their study and the evidence they quote of other dissident authors, their figure is still far from universally accepted. Their result and the values of D and R from which it is derived are given in the first line of **Table 4**.

| | D (mm) | R (mm) | θ (0.0001 rad) | \mathcal{N} |
|------------------|-------------------|------------------|-----------------------|------------------|
| 1) BTDR | 1.365 ± 0.015 | 77.493 | | 356.71 |
| 2) Weighted mean | 1.363 ± 0.021 | 77.09 ± 0.28 | | 354.8 ± 5.6 |
| 3) 6 sections | | 77.34 ± 1.09 | 8.843 ± 0.265 | 355.2 ± 10.7 |
| 4) 4 sections | | 77.06 ± 0.08 | 8.896 ± 0.093 | 353.1 ± 3.7 |
| 5) 2 sections | | 77.35 ± 0.32 | 8.915 ± 0.053 | 352.3 ± 1.5 |

Table 4. Collected results of BTDR and the present study.

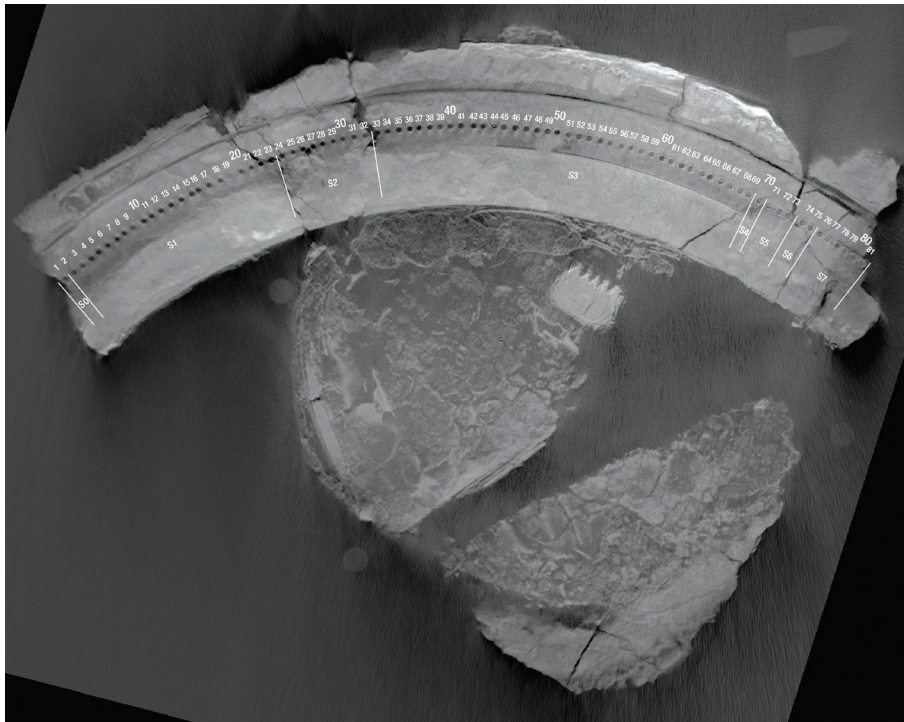
In the present study we have reexamined the BTDR analysis. We find a number of disagreements with their methodology, particularly concerning their treatment of errors, and have repeated their analysis using their data on the (x, y) coordinates of the 81 extant holes, but with our own adjustments to obtain the results given in the second line of **Table 4**.

We then re-formulated the problem in terms of θ instead of D , giving equal weight to each x and each y value, and solving all the equations simultaneously by the method of least squares. The somewhat disappointing (because of the larger SEs) results are given in the third line of **Table 4**.

Nevertheless, the results provided information on the movement, or lack of movement, between sections that allowed us to combine sections with consequent improvement in the conditioning of the equations and diminution of SEs, which has led to the results given in lines 4 and 5 of **Table 4**.

These, then, are our results, with that given in line 5 our best estimate. The progression that led to this solution has been summarized here and detailed in the preceding sections. That the 2-section model reported in line 5 of **Table 4** represents the best overall fit to the data is confirmed by the very small SEs. The value of \mathcal{N} has to be integral and the SE of 1.5 indicates that there is less than a 5% probability that \mathcal{N} is not one of the six values in the range 350–355. The chances of \mathcal{N} being as high as 365 are less than 1 in 10,000.⁶

While other contenders cannot be ruled out, of the two values that have been proposed for \mathcal{N} on astronomical grounds, that of BTDR (354) is by far the more likely.



Fragment C, composite CT image of holes.
Reproduced from *HJ*, March 2021.

REFERENCES

1. Freeth, Tony; Higgon, David; Dacanalís, Aris; Macdonald, Lindsay; Georgakopoulou, Mytro and Wojcik, Adam, 'A Model of the Cosmos in the ancient Greek Antikythera Mechanism,' *Nature Portfolio Scientific Reports*, 2021, <www.nature.com/articles/s41598-021-84310-w> last accessed 26 February 2024. See also Jones, A., 'A Portable Cosmos: Revealing the Antikythera Mechanism, Scientific Wonder of the Ancient World' (Oxford University Press, 2017); and Freeth *et al.*, <www.vimeo.com/518734183> last accessed 26 February 2024.
2. Budiselic, C., Thoeni, A. T., Dubno, M. and Ramsey, A. T., 'The Antikythera Mechanism, Evidence of a Lunar Calendar – Part 1 of 2', *Horological Journal*, vol. 163 (March 2021), pp104–112. See also: <<https://doi.org/10.7910/DVN/VJGLVS>> and <<https://bhi.co.uk/antikytheramechanism>> both links accessed 26 February 2024.
3. Malin, S. R. C., Barraclough, D. R. and Hodder, Barbara M., 1982, 'A compact algorithm for the formation and solution of normal equations', *Computers & Geosciences*, 8, 355–358.
4. Harvard Dataverse repository <<https://dataverse.harvard.edu/dataverse/amelc>> last accessed 26 February 2024.
5. Also available at <<https://doi.org/10.7910/DVN/VJGLVS/RTURPj>> last accessed 26 February 2024.
6. See, for example, 'Table 1' on p320 of *Mathematics of Statistics, Part 1*, Kennard, J. F. and Keeping, E. S. (D van Nostrand Company, Inc, 1954, 3rd edition), explanation on pp110–111.



Stuart Malin



R. J. Dickens

The authors joined the staff of the Royal Greenwich Observatory in Herstmonceux in 1958 as Assistant Experimental Officers. They worked their way up through the Scientific Civil Service grades to the coveted rank of Senior Principal Scientific Officer (Individual Merit); coveted because the 'Individual Merit' gave almost total academic freedom with no administrative responsibility.

Both are Fellows of the Royal Astronomical Society and have served on its Council. Together they have amassed 174 years, five degrees – including three doctorates – and various academic appointments, including Visiting Reader at Sussex University, Visiting Professor at the Universities of Bristol, Cairo, Cardiff, and U. C. London, and a Personal Chair at Boğaziçi Üniversitesi Istanbul.

In addition, R. J. Dickens has worked on secondment to the USA as Carnegie Fellow at the Mount Wilson and Palomar Observatories; in Australia (at the Anglo-Australian Observatory); in South Africa (at the Royal Observatory, Cape and the Radcliffe Observatory, Pretoria), and as staff member at Rutherford Appleton Laboratory (Head of the Starlink astronomical computing service) and the Wildfowl and Wetlands Trust.

Stuart Malin has worked in South Africa as Cape Observer at the Radcliffe Observatory; in the USA (Green Scholar at Scripps Institution of Oceanography; Visiting Scientist at National Center for Atmospheric Research); Australia (Visiting Scientist at Sydney University); Canada (Dept. of Energy Mines and Resources); India (Guest of British Council) and Japan (Tokyo Institute of Technology). He has also worked as a staff member at British Geological Survey (Head of Geomagnetism Unit); National Maritime Museum (Director of Old Royal Observatory, Greenwich) and Dulwich College. He is a Fellow of the Institute of Physics, Liveryman of the Worshipful Company of Clockmakers and a proud holder of the National Licensee's Certificate.